Comparative Study of Ring-Opening Polymerization of *L*-Lactide and *ε*-Caprolactone Using Zirconium Hexadentate Bis(aminophenolate) Complexes as Catalysts

Hsiu-Wei Ou,[a] Michael Y. Chiang,[b] Jaya Kishore Vandavasi,[a] Wei-Yi Lu,[a] Yen-Jen Chen,[a] Hsi-Ching Tseng,[a] Yi-Chun Lai,[a] Hsuan-Ying Chen*[a]

[a]*Department of Medicinal and Applied Chemistry, Kaohsiung Medical University, Kaohsiung 80708, Taiwan, R.O.C.*

[b] *Department of Chemistry, National Sun Yat-sen University, Kaohsiung, Taiwan, 80424, R.O.C.*

Department of Medicinal and Applied Chemistry, Kaohsiung Medical University, Kaohsiung 80708, Taiwan, R.O.C.

Electronic supplementary information available: Polymer characterization data, and details of the kinetic study.

Table of Contents

Table S1. The variations of [PCL] in ROP process with Zr complexes in $CDCl_3$1 mL, [CL] = 1.0 M in a sealed NMR tube at 100 °C. [CL] : [cat.] = 100:1

OMe		F		NMe2		Bn	
Time(h)	Conv.(%)	Time(h)	Conv.(%)	Time(h)	Conv.(%)	Time(h)	Conv.(%)
0	0	0	0	0	0	0	0
5	20.79	4	38.79	4	20.10	4	29.36
9	24.87	5	47.64	5	23.23	5	34.99
20	46.72	6	50.70	9	32.00	6	37.40
28	61.12	7	54.14	17	49.47	7	40.36
32	65.24	9	60.83	20	58.33	9	46.10
42	74.25	11	67.05	28	72.46	11	54.98
52	80.99			32	73.64	14	61.13
60	83.64					17	68.73
70	87.36					20	72.39
85	90.28					28	85.93
k_{obs} (error), R^2							
0.02816(95), 0.99		0.09886(674), 0.99		0.04235(161), 0.99		0.06617(181), 0.99	

Fu		Th		Py	
Time(h)	Conv.(%)	Time(h)	Conv.(%)	Time(h)	Conv.(%)
0	0	0	0	0	0
4	49.39	4	49.40	4	3.89
5	53.59	5	53.01	5	5.94
6	57.41	6	58.07	9	9.88
7	60.27	7	62.54	20	24.66
9	65.13	9	70.82	28	36.75
11	69.91	11	74.66	32	41.31
14	77.32	14	82.69	42	52.81
17	81.73	17	87.74	52	61.71

	20	91.24	60	67.68
			70	74.11
			85	81.20
			100	86.46
			120	90.42
k_{obs} (error), R^2				
0.09162(734), 0.98	0.11617(349), 0.99		0.02021(27), 0.99	

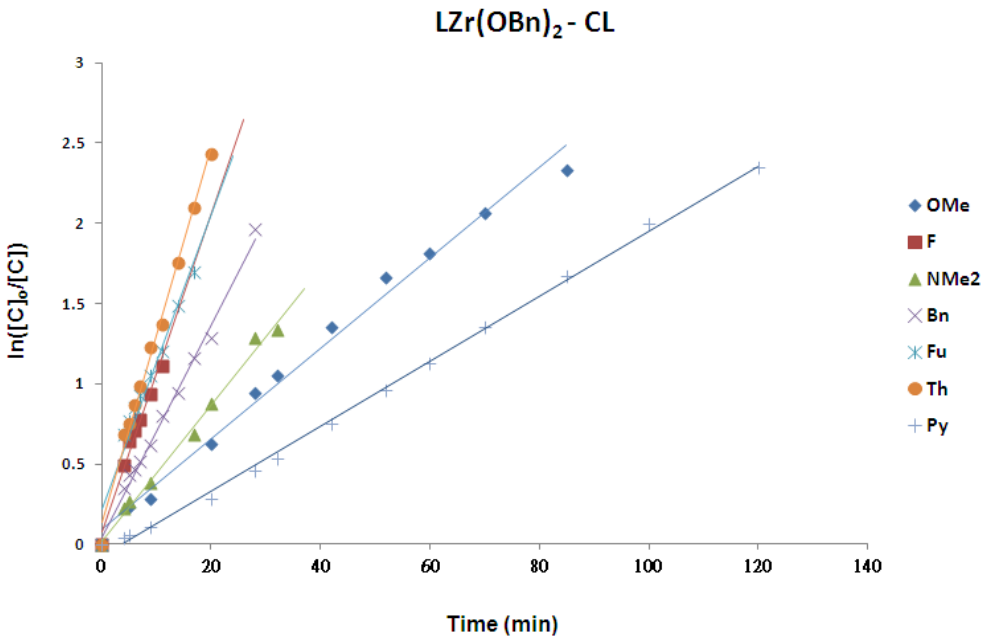

Figure S1 First-order kinetic plots for CL polymerizations with time with different Zr complexes

Table S2 The variations of [PLA] in ROP process with Zr complexes in $CDCl_3$ 1 mL, [CL] = 1.0 M in a sealed NMR tube at 100 °C

OMe		F		NMe2		Py	
Time(h)	Conv.(%)	Time(h)	Conv.(%)	Time(h)	Conv.(%)	Time(h)	Conv.(%)
0	0	0	0	0	0	0	0
0.066667	11.96	6	30.39	8	34.44	0.016667	10.29
0.116667	13.10	8	32.42	14	47.41	0.033333	12.91
0.25	17.26	14	43.73	19	53.76	0.05	15.06
0.5	21.30	19	51.50	23.25	62.98	0.083333	17.47
0.75	25.60	23.25	55.84	28	66.79	0.1	18.51
1.25	38.49	28	59.19	35.75	72.49	0.2	25.39
1.75	46.77	35.75	66.66	41	76.26	0.216667	27.42
2.25	55.31	41	71.87	49	82.76	0.4	40.25
2.75	61.46					0.6	52.08
3.5	70.55					1.0	72.06
k_{obs} (error), R^2							
0.3264(85), 0.99		0.0281(17), 0.99		0.0337(15), 0.99		1.1741(363), 0.99	

Fu		Th		Bn	
Time(h)	Conv.(%)	Time(h)	Conv.(%)	Time(h)	Conv.(%)
0	0	0	0	0	0
0.066667	12.35	2	21.54	6	30.91
0.116667	15.60	3	27.67	8	31.99
0.25	22.17	6	30.01	14	38.68
0.5	26.60	8	37.89	19	51.19
0.75	31.56	14	46.79	23.25	55.47
1.25	43.32	19	52.53	28	60.71
1.75	53.61	23.25	56.14	35.75	68.88

2.25	58.63	35.75	68.75	41	72.57
2.75	63.22	41	73.77		
3.5	69.71	49	77.02		
		56	80.05		
		k_{obs} (error), R^2			
0.3238(153), 0.99		0.0265(12), 0.99		0.0297(15), 0.99	

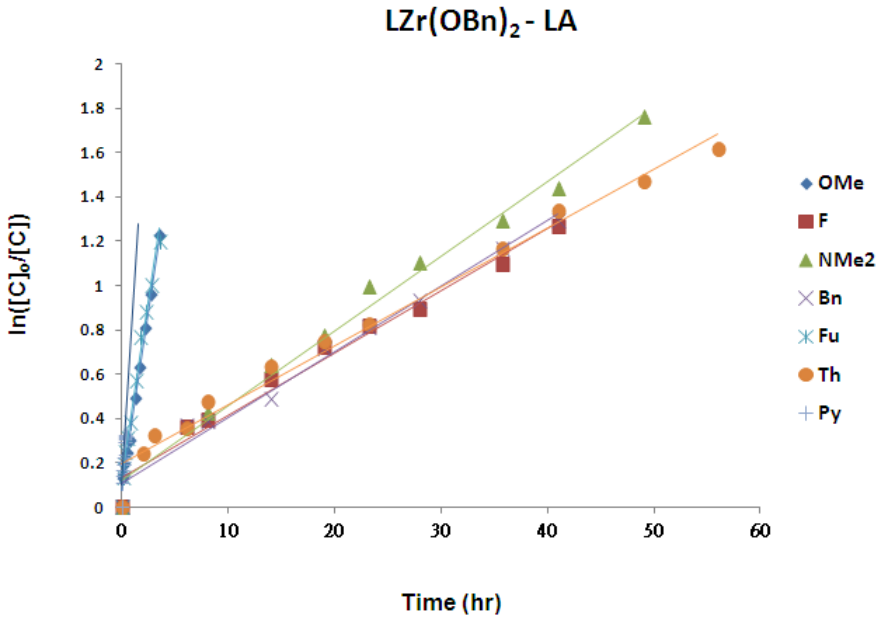

Figure S2 First-order kinetic plots for LA polymerizations in $CDCl_3$ with time with different Zr complexes

Details of the Kinetic Study of ε-CL and *L*-Lactide Polymerization

A typical kinetic study was conducted to establish the reaction order with respect to monomer and $\mathbf{L^{OMe}Zr(OBn)_2}$. For CL polymerization, ε-caprolactone (1.14 g, 2.0 M) was added to a solution of $\mathbf{L^{OMe}Zr(OBn)_2}$ (0.20, 0.16, 0.12, 0.08 M) in CH_2Cl_2 (5 mL), respectively. The solution was then stirred at room temperature under nitrogen. At the indicated time intervals, 0.05 mL aliquots were removed, trapped with $CDCl_3$ (1 mL), and analyzed by ^{1}H NMR. The ε-caprolactone concentration [CL] was determined by integrating the triplet methylene peak of CL at 4.20 ppm and the triplet methylene peak of polylactone at 4.00 ppm. As expected, plots of $\ln([CL]_0/[CL])$ vs. time for a wide range of [$\mathbf{L^{OMe}Zr(OBn)_2}$] are linear, indicating the usual first order dependence on monomer concentration (Figure S3, Table S3). Thus, the rate expression can be written as $-d[CL]/dt = k_{app}[CL]^1[\mathbf{L^{OMe}Zr(OBn)_2}]^x = k_{obs}[CL]^1$, where $k_{obs} = k_{app}[\mathbf{L^{OMe}Zr(OBn)_2}]^x$. Plotting ln *k*obs vs ln[$\mathbf{L^{OMe}Zr(OBn)_2}$] allows us to determine x, the order in [$\mathbf{L^{OMe}Zr(OBn)_2}$]. From the slope of the fitted line as shown in Figure S4, the rate constant k is 0.0015 M^{-2} s^{-1}. Therefore, on the basis of this analysis, $x = 2$. The reaction is first order in CL and second order in[$\mathbf{L^{OMe}Zr(OBn)_2}$], and the overall rate equation is $-d[CL]/dt = k[CL]^1[\mathbf{L^{OMe}Zr(OBn)_2}]^2$.

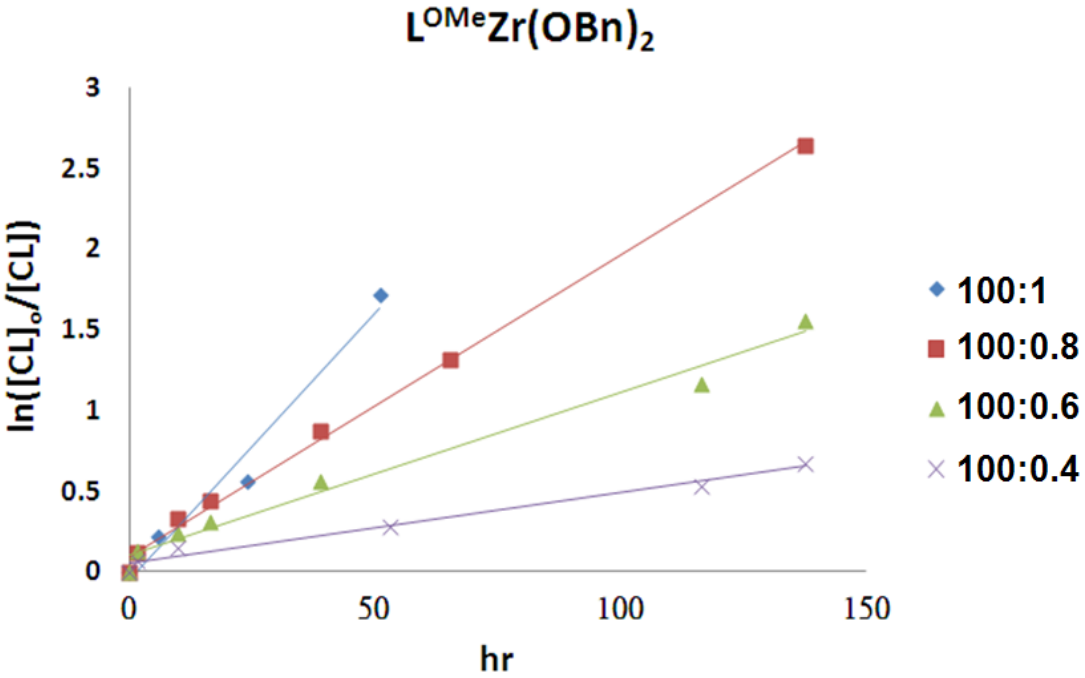

Figure S3 First-order kinetic plots for CL polymerizations with time in CH_2Cl_2 (5 mL) with different concentration of $L^{OMe}Zr(OBn)_2$.

Table S3 The variations of [PCL][a] in ROP process with a wide range of $L^{OMe}Zr(OBn)_2$ in CH_2Cl_2 5 mL, [CL] = 2.0 M at room temperature.

100:4		100:6		100:8		100:10	
Time(h)	Conv.(%)	Time(h)	Conv.(%)	Time(h)	Conv.(%)	Time(h)	Conv.(%)
0	0	0	0.00	0	0.00	0	0
1.5	6.86	1.5	11.92	1.5	10.87	6	19.28
10	13.62	10	21.29	10	27.95	24	43.04
53	24.67	16.5	26.76	16.5	35.88	51	82.00
116.5	41.29	39	42.93	39	58.22		
137.75	48.95	116.5	68.86	65.5	73.04		
		137.75	78.90	137.75	92.89		
k_{obs} (error), R^2							
0.0044(3), 0.99		0.0101(6), 0.99		0.0186(5), 0.99		0.0329(38), 0.98	

[a] Obtained from ^1H NMR analysis.

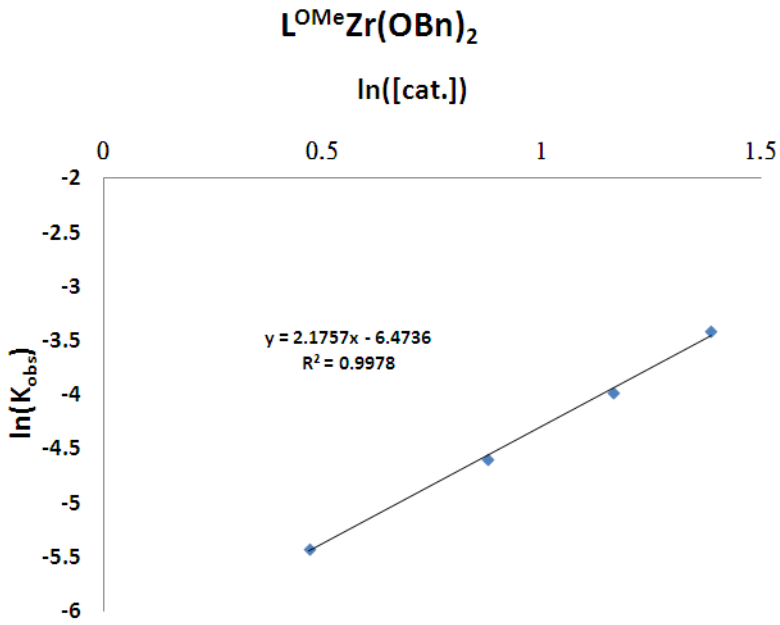

Figure S4 Linear plot of lnk_{obs} vs ln[$L^{OMe}Zr(OBn)_2$] for the polymerization of CL with [CL] = 2.0 M in toluene (5 mL) at at room temperature.

For LA polymerization, *L*-lactide (0.18 g, 1.25 mmol, 1.25 M) was added to a solution of **$L^{OMe}Zr(OBn)_2$** (0.025, 0.05, 0.075, 0.10 M) in $CDCl_3$ (1 mL), respectively. The solution was set in the NMR tube and sealed at 100°C. At the indicated time intervals, the tube was analyzed by ^{1}H NMR. The *L*-lactide concentration [LA] was determined by integrating the quartet methine peak of LA at 5.00 ppm and the quartet methine peak of polylactic acid at 5.20 ppm. As expected, plots of $\ln[LA]_0/\ln[LA]$ vs. time for a wide range of [**$L^{OMe}Zr(OBn)_2$**] are linear, indicating the usual first order dependence on monomer concentration (Figure S5, Table S4). Thus, the rate expression can be written as $-d[LA]/dt = k_{app}[LA]^1[\mathbf{L^{OMe}Zr(OBn)_2}]^x = k_{obs}[LA]^1$, where $k_{obs} = k_{app}[\mathbf{L^{OMe}Zr(OBn)_2}]^x$. A plot of k_{obs} vs. **$L^{OMe}Zr(OBn)_2$** (Figure S6) is linear, indicating the order of **[$L^{OMe}Zr(OBn)_2$]** ($x = 1$) and k_{app} which is 1.6636 $M^{-1}min^{-1}$.

Figure S5. First-order kinetic plots for LA polymerizations with time in $CDCl_3$ (1 mL) with different concentration of **$L^{OMe}Zr(OBn)_2$**.

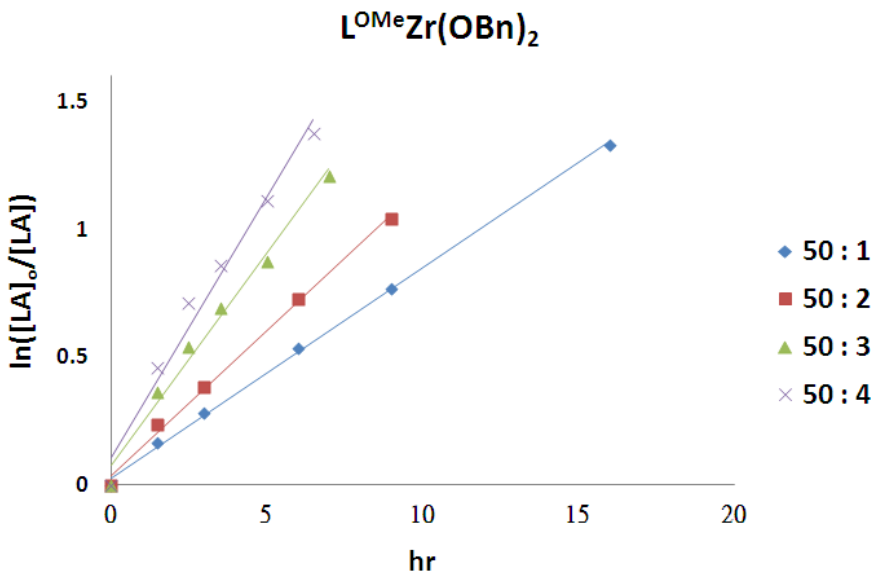

Table S4 The variations of [PLA][a] in ROP process with a wide range of **$L^{OMe}Zr(OBn)_2$** in $CDCl_3$ 1 mL, [LA] = 1.25 M at 100 °C.

50:1		50:2		50:3		50:4	
Time(h)	Conv.(%)	Time(h)	Conv.(%)	Time(h)	Conv.(%)	Time(h)	Conv.(%)
0	0	0	0	0	0	0	0
1.5	15.27	1.5	21.11	1.5	30.27	1.5	36.69
3	24.70	3	31.80	2.5	41.78	2.5	50.89
6	41.48	6	51.63	3.5	50.02	3.5	57.56
9	53.50	9	64.69	5	58.25	5	67.03
16	73.57			7	70.06	6.5	74.63
k_{obs} (error), R^2							
0.08188(143), 0.99		0.11343(41), 0.99		0.16535(1013), 0.99		0.20321(1574), 0.99	

[a] Obtained from ^1H NMR analysis.

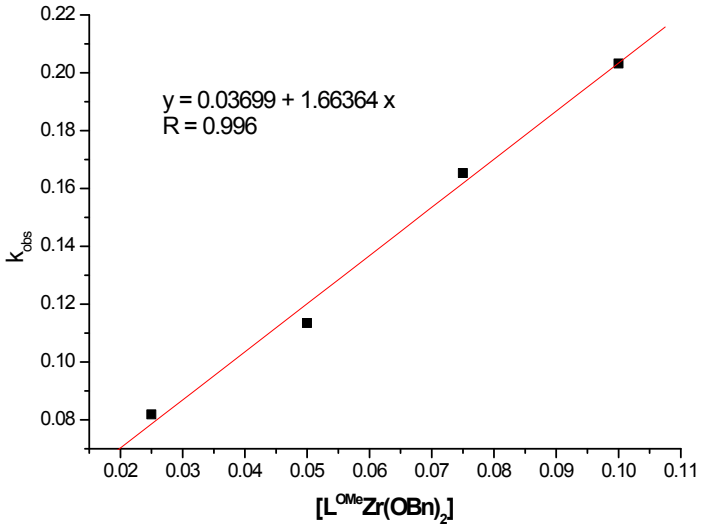

Figure S6. Linear plot of k_{obs} vs [**$L^{OMe}Zr(OBn)_2$**] for the polymerization of LA with [LA] = 1.25 M in $CDCl_3$ (1 mL) at 100 °C.

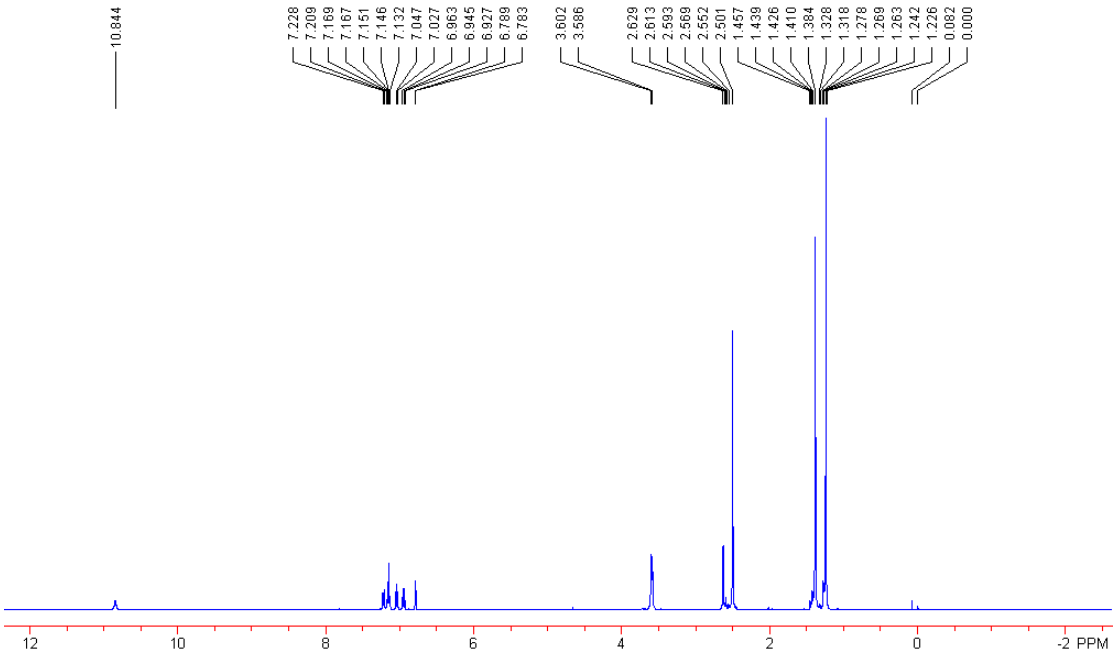

Figure S7. The ^{1}H NMR spectrum of $L^{NMe2} - H_2$

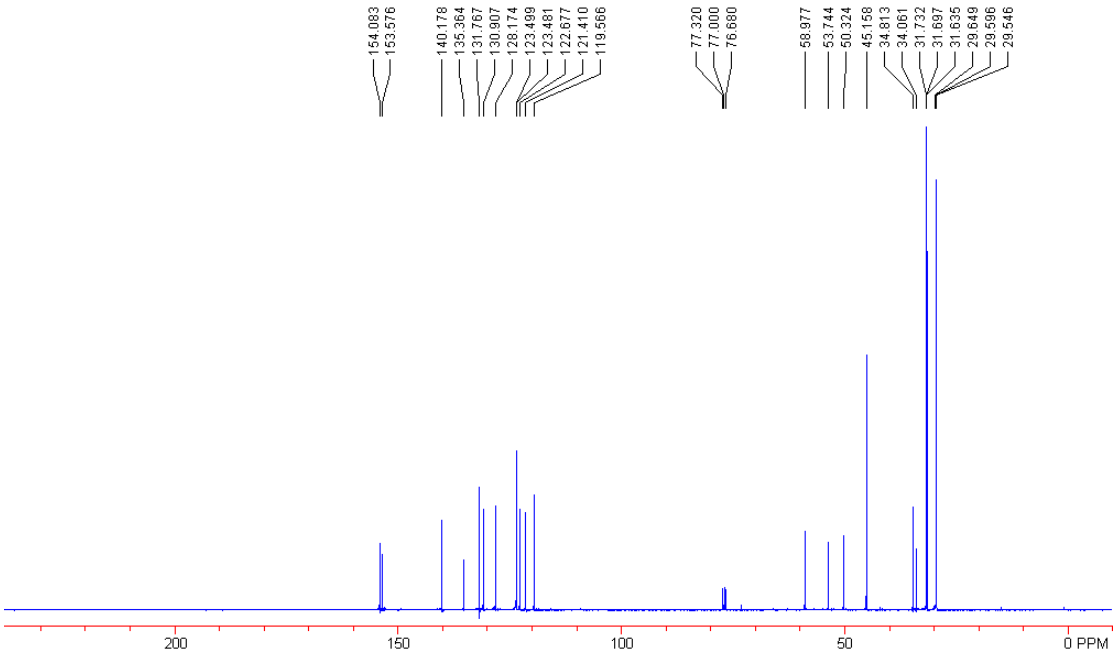

Figure S8. The ^{13}C NMR spectrum of $L^{NMe2} - H_2$

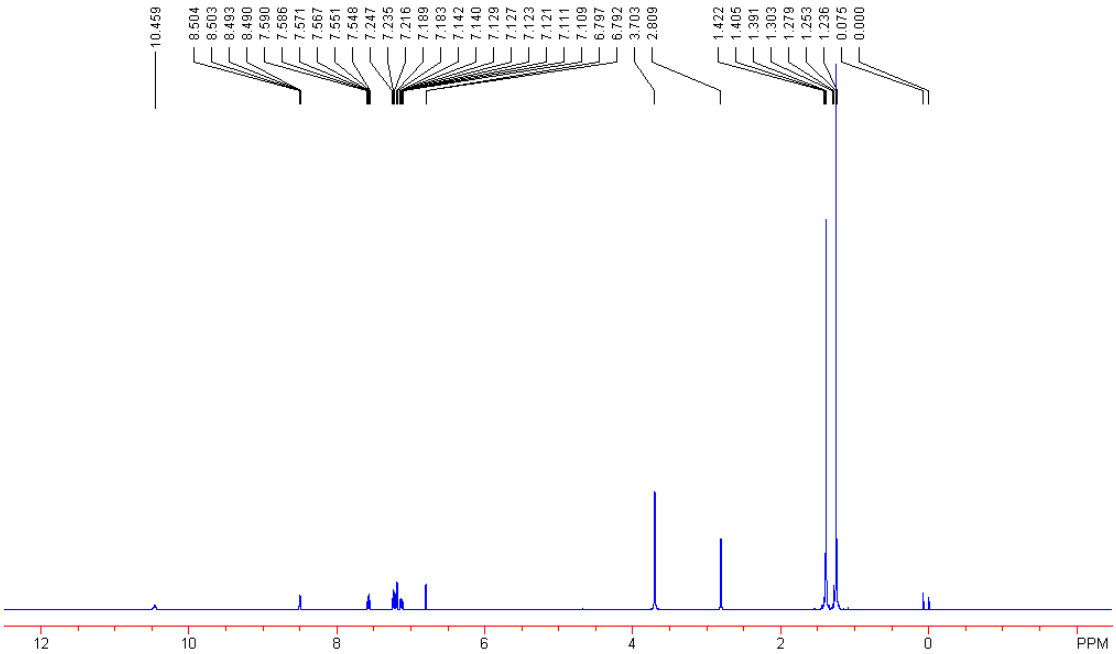

Figure S9. The ^{1}H NMR spectrum of $L^{Py} - H_2$

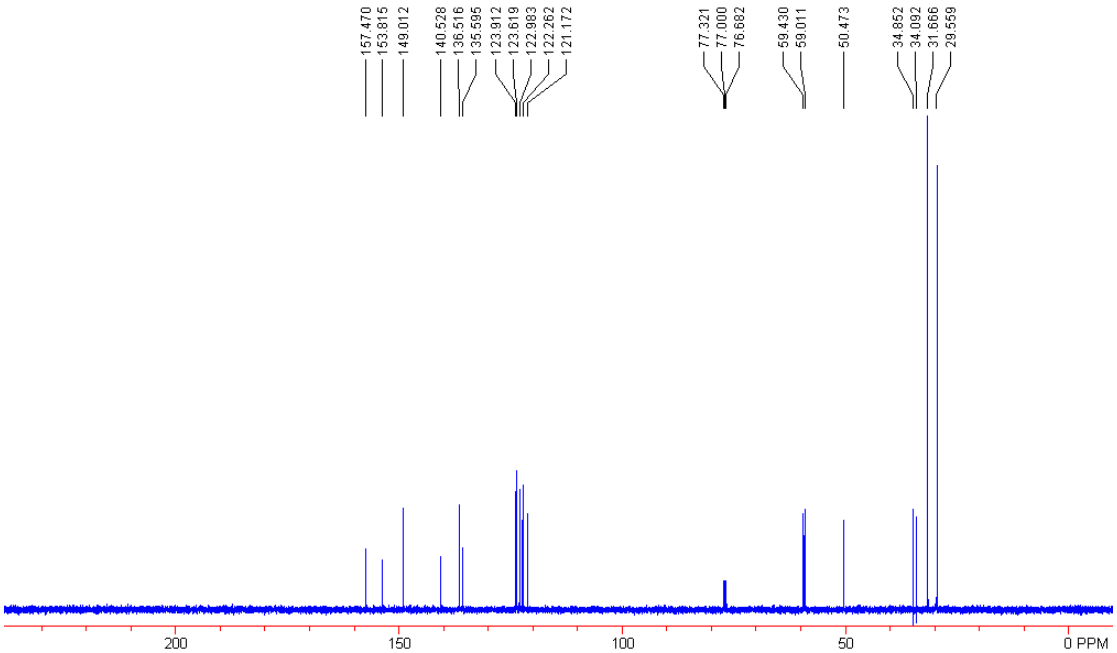

Figure S10. The ^{13}C NMR spectrum of $L^{Py} - H_2$

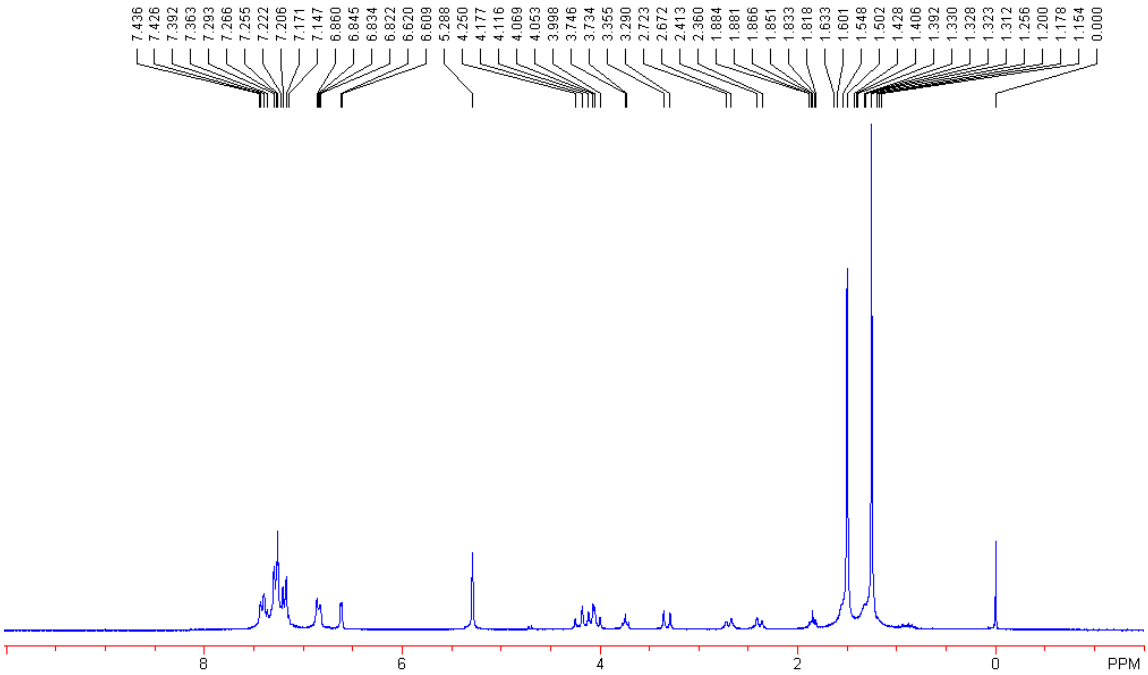

Figure S11. The ^{1}H NMR spectrum of $\mathbf{L^{Bn}Zr(OBn)_2}$

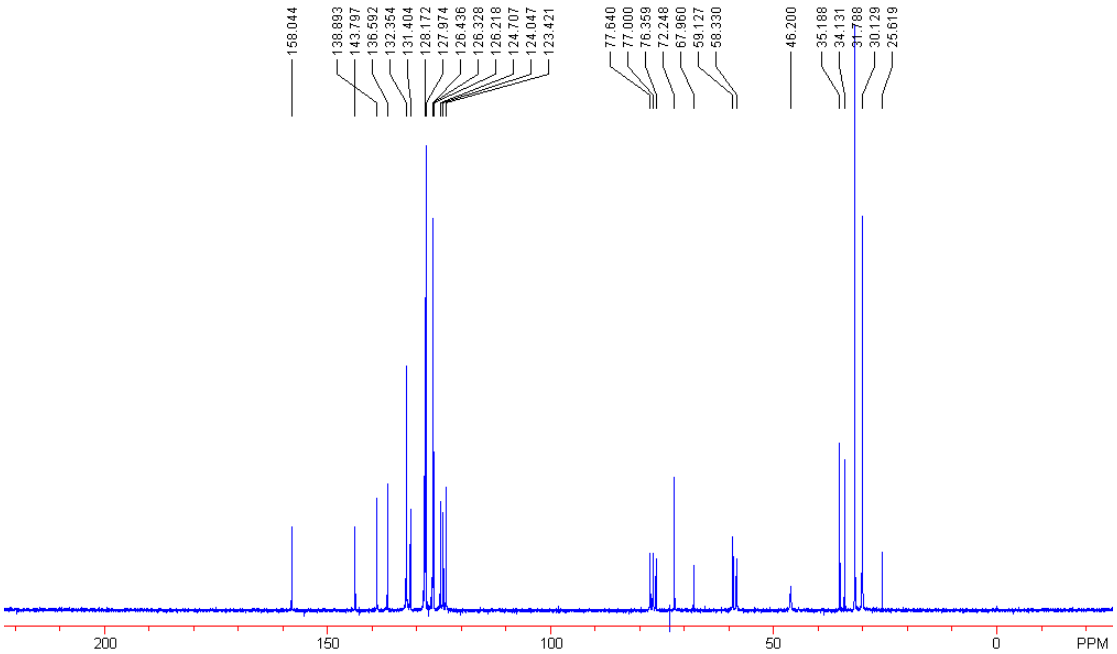

Figure S12. The ^{13}C NMR spectrum of $\mathbf{L^{Bn}Zr(OBn)_2}$

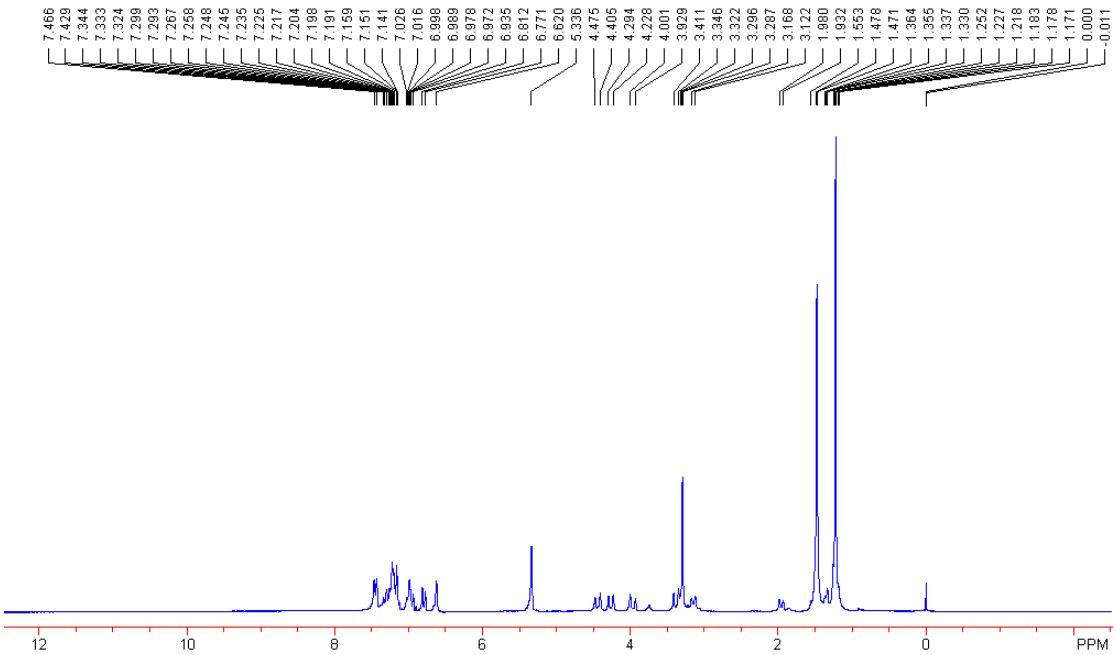

Figure S13. The ^{1}H NMR spectrum of $\mathbf{L^{OMe}Zr(OBn)_2}$

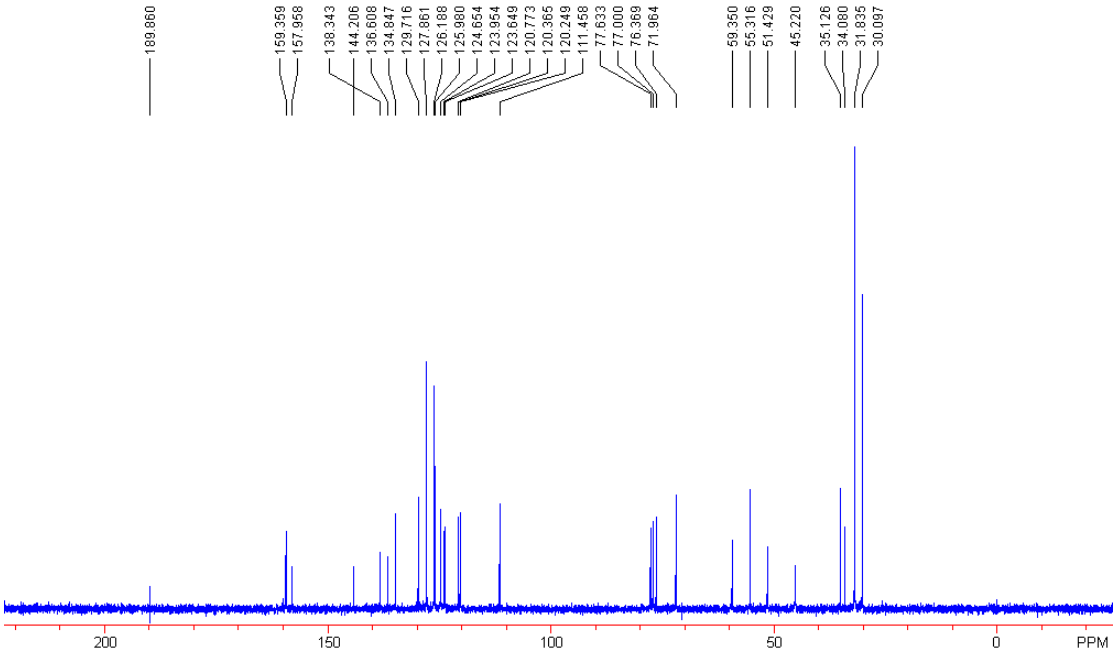

Figure S14. The ^{13}C NMR spectrum of $\mathbf{L^{OMe}Zr(OBn)_2}$

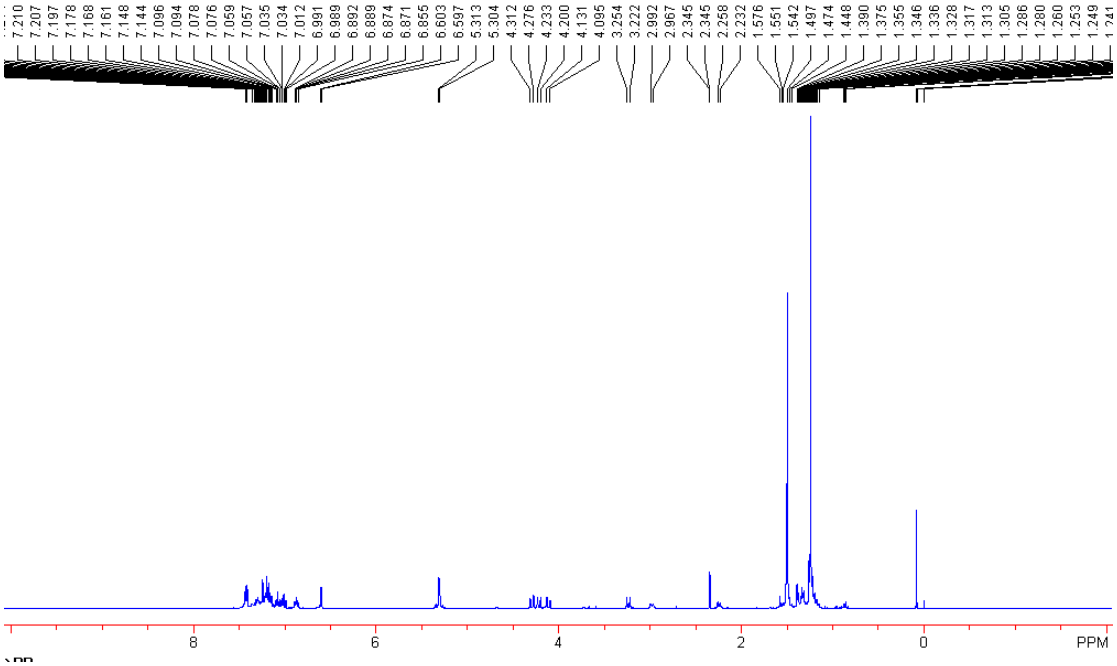

Figure S15. The ^{1}H NMR spectrum of $\mathbf{L^{F}Zr(OBn)_2}$

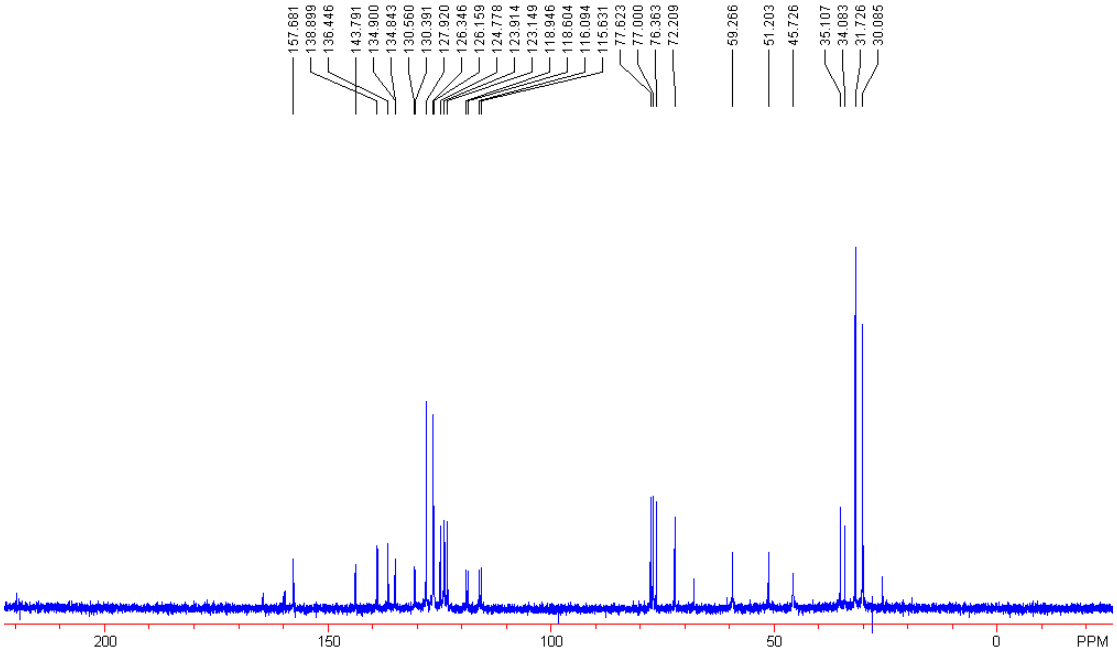

Figure S16. The ^{13}C NMR spectrum of $\mathbf{L^{F}Zr(OBn)_2}$

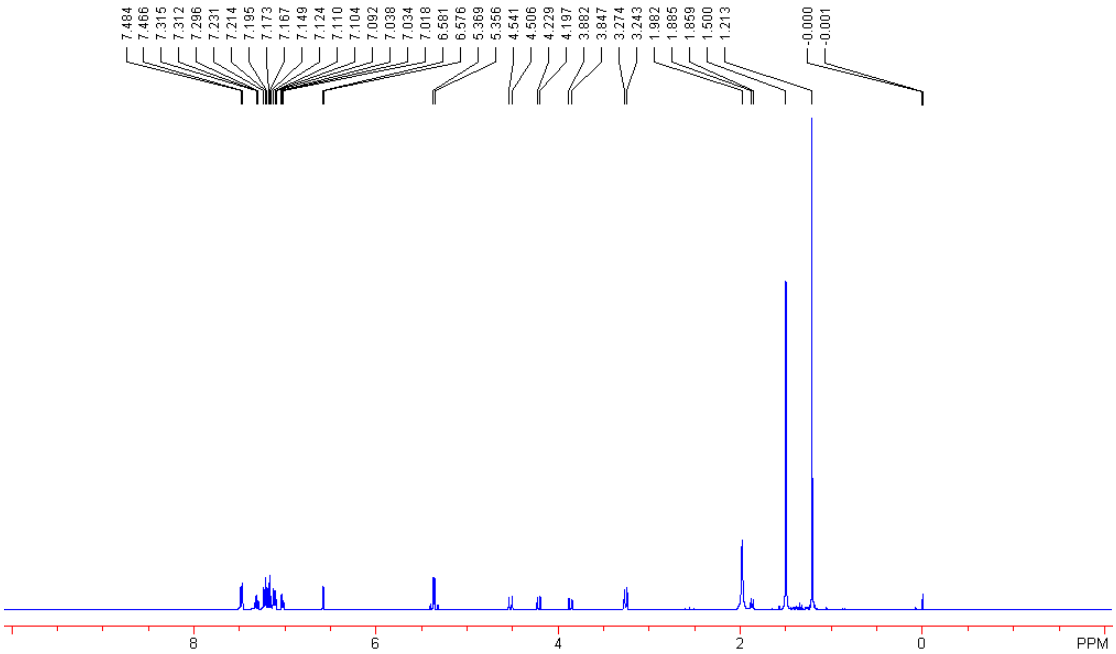

Figure S17. The ^{1}H NMR spectrum of $\mathbf{L^{NMe2}Zr(OBn)_2}$

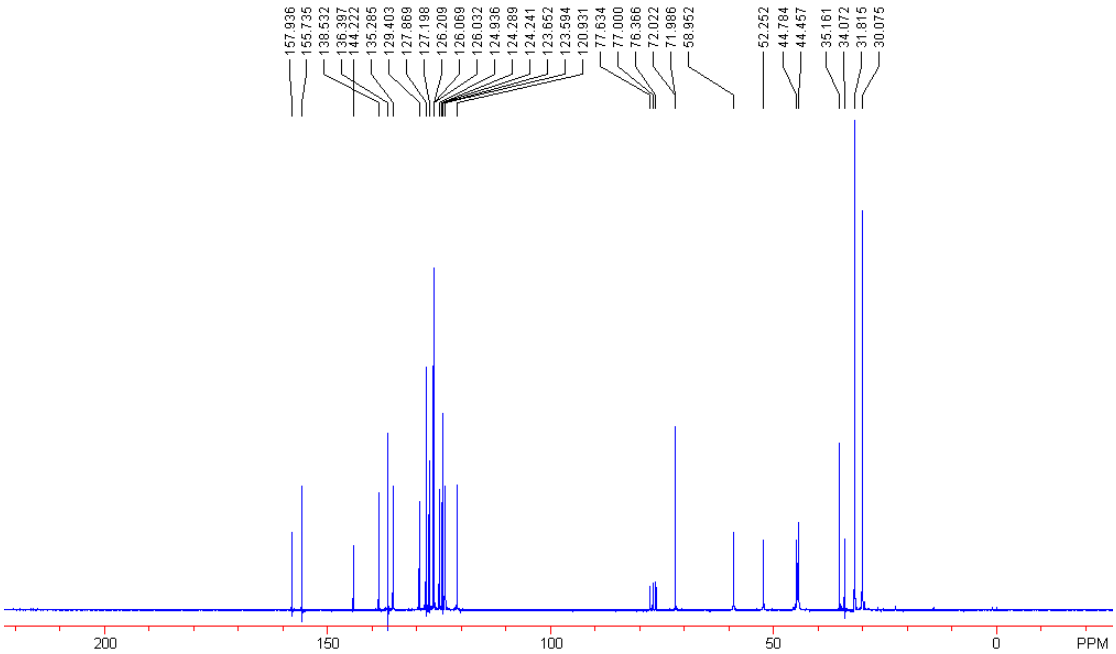

Figure S18. The ^{13}C NMR spectrum of $\mathbf{L^{NMe2}Zr(OBn)_2}$

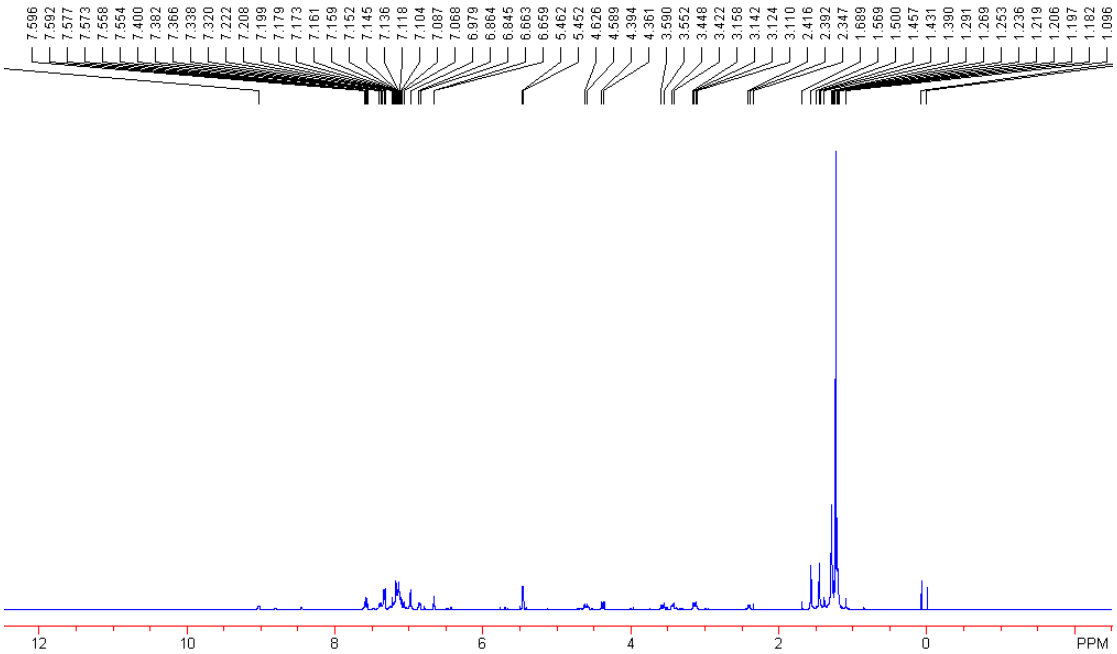

Figure S19. The ^{1}H NMR spectrum of $\mathbf{L^{Py}Zr(OBn)_2}$

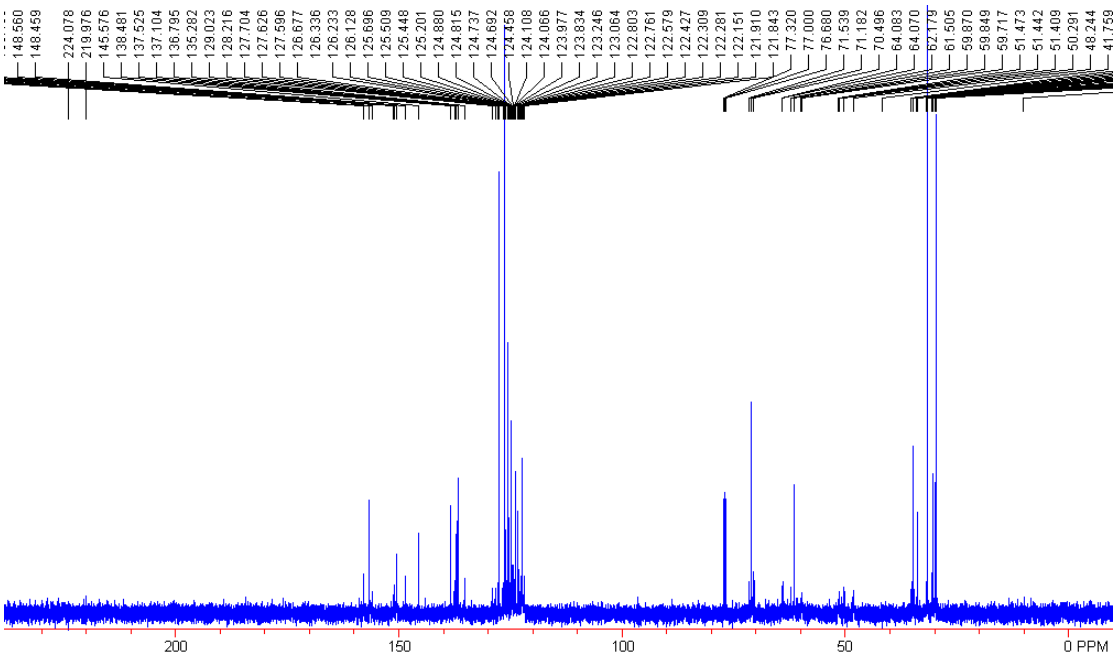

Figure S20. The ^{13}C NMR spectrum of $\mathbf{L^{Py}Zr(OBn)_2}$

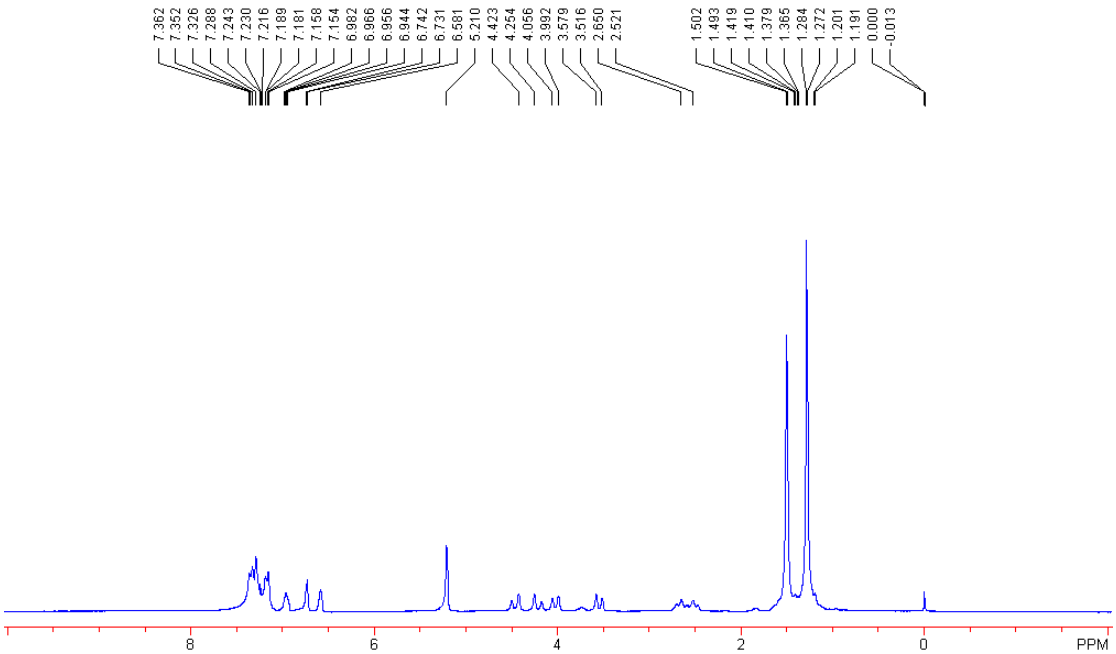

Figure S21. The ^{1}H NMR spectrum of $\mathbf{L^{Th}Zr(OBn)_2}$

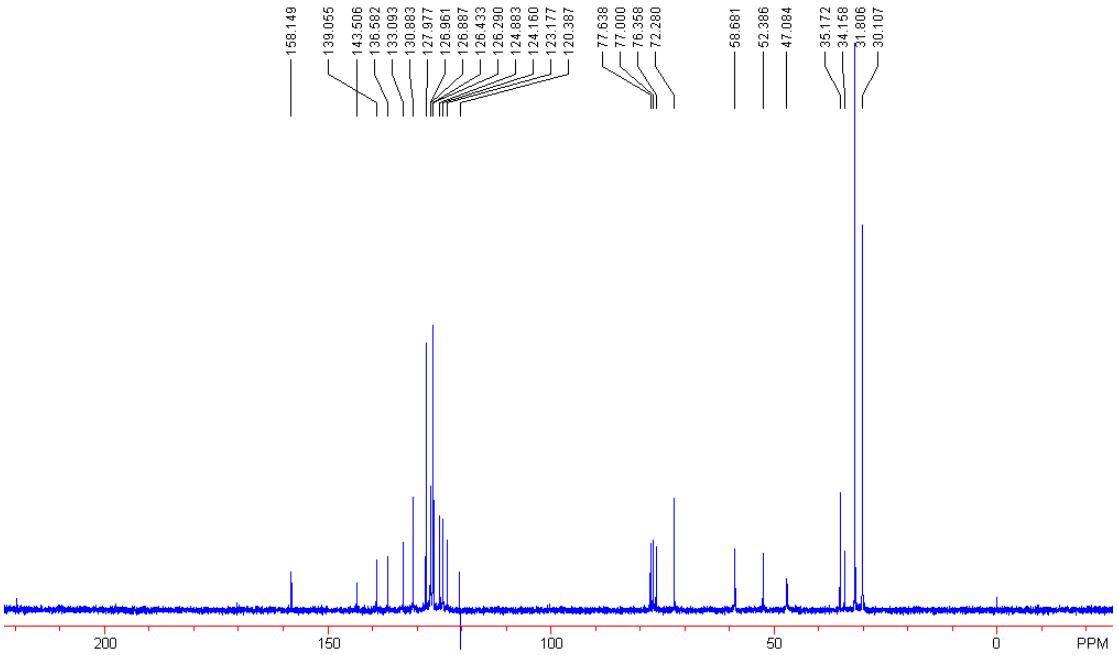

Figure S22. The ^{13}C NMR spectrum of $\mathbf{L^{Th}Zr(OBn)_2}$

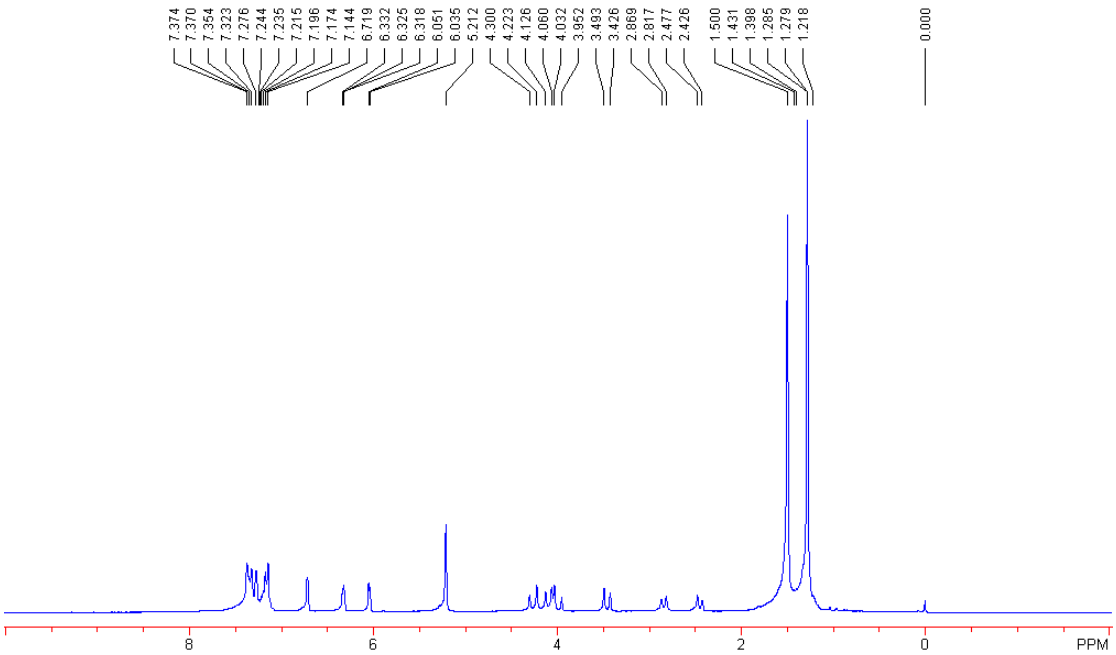

Figure S23. The ^{1}H NMR spectrum of $\mathbf{L^{Fu}Zr(OBn)_2}$

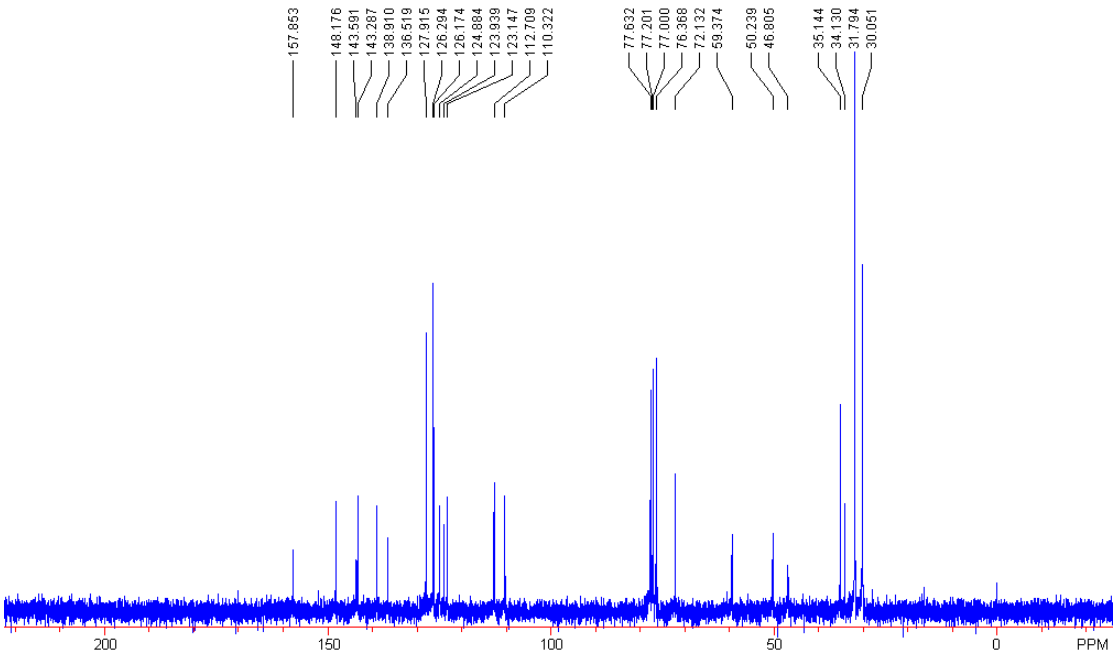

Figure S24. The ^{13}C NMR spectrum of $\mathbf{L^{Fu}Zr(OBn)_2}$